

## Energy and environmental nanotechnology in conductive paper and textiles

Liangbing Hu and Yi Cui\*

Received 19th August 2011, Accepted 3rd January 2012

DOI: 10.1039/c2ee02414d

Paper and textiles have been used ubiquitously in our everyday lives, such as books and newspapers for propagating information, clothing and packaging. In this perspective, we will summarize our recent efforts in exploring these old materials for emerging energy and environmental applications. The motivations and challenges of using paper and textiles for device applications will be discussed. Various types of energy and environmental devices have been demonstrated including supercapacitors, Li-ion batteries, microbial fuel cells and water filters. Due to their unique morphologies, paper and textile-based devices not only can be fabricated with simple processing, but also show outstanding device performance. Being renewable and earth-abundant materials, paper and textiles could play significant roles in addressing future energy and environmental challenges.

### 1. Introduction

#### 1.1 Paper and textiles: ancient materials from renewable resources

Paper and textiles are versatile materials, which are made of fibers with typical diameters of  $\sim 20\ \mu\text{m}$ .<sup>1</sup> Depending on the type of materials for making paper and textiles, the fiber diameter varies. With a fiber network structure, paper and textiles are typically flexible and porous. There is a range of raw materials for making paper and textiles, such as wood, cotton, grass, wool *etc.*, which are earth-abundant and renewable. By far, paper is the cheapest flexible substrate.<sup>2</sup> These microfibers normally have a hierarchical structure, *i.e.* they are made of smaller nanofibers with diameters in the range of tens of nanometers. This morphology, together with their rich surface chemistry and reliable stability, allow the wide use of paper and textiles in a variety of applications, such as writing, painting, packaging and clothing. The making and processing of paper and textiles has a long history, and the roll-to-roll

manufacturing infrastructure is mature and advanced. If new applications can be identified, this will pave the way for utilizing paper and textiles in emerging technologies.

#### 1.2 Electronic devices made of paper and textiles

Low cost, flexible macroelectronics using roll-to-roll fabrication methods have attracted much attention recently as a complement to high-performance Si-based electronics. Paper electronics have been a dream of next-generation electronics. As a low cost substrate with excellent printing compatibilities, paper has attracted much research attention recently. Whitesides *et al.* demonstrated a much simpler way to fabricate 3D microfluidic devices using paper as the substrate (Fig. 1(a)).<sup>3</sup> The thin film transistor (TFT) is an essential component for active devices for integrated functional devices, such as flexible electronics. Due to paper's intrinsically large surface roughness, it is challenging to build electronic devices on its surface due to the fact that the thickness of the dielectric layer is typically much less than the surface roughness of paper. A simple approach is to smooth the paper surface by adding another layer of polymers and build devices on top of the treated paper surface.<sup>4,5</sup> However, this

Department of Materials Science and Engineering, Stanford University, California, 94305, USA. E-mail: yicui@stanford.edu

### Broader context

The energy and environmental challenges we face are daunting, which call for high-performance devices that can be manufactured with low-cost processing and earth-abundant materials. Paper and textiles have been widely used by mankind for over a thousand years. These materials are renewable, earth-abundant, and have interesting properties. Nanotechnology has been the focus of development in the past two decades, creating interesting nanomaterials and revealing exciting properties. The union between nanotechnology and paper and textile technology presents new opportunities towards high performance and low-cost energy and environmental technologies. Recently, there has been steady progress in utilizing paper and textiles as substrates for energy and environmental devices. Often, nanomaterials are incorporated in these traditional paper and textile materials. Devices with outstanding performances have been demonstrated, such as supercapacitors, batteries, microbial fuel cells and water filters.

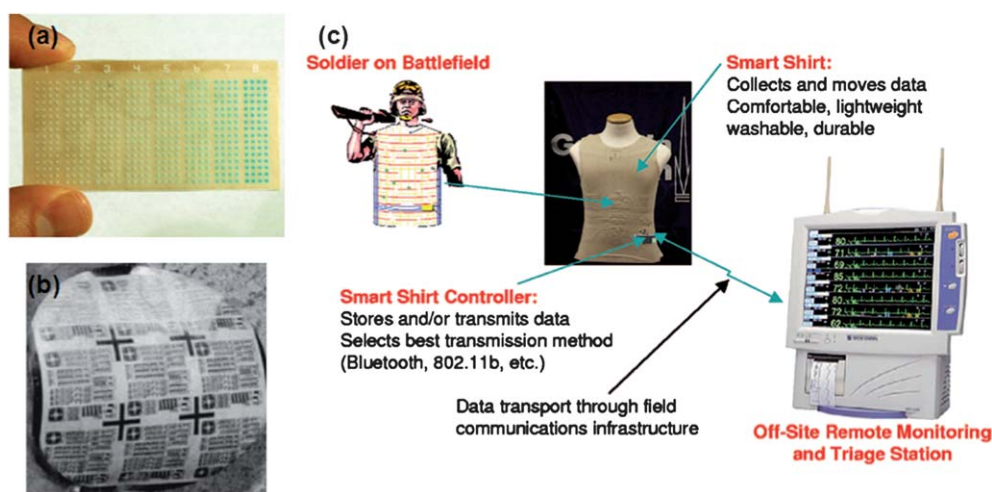


**Fig. 1** (a) A photograph of a paper-based 3D microfluidic device. (b) A photograph of pentacene TFTs and integrated circuits on paper. (c) The smart shirt in the field.<sup>3,13</sup>

approach will not be able to take advantage of paper as an excellent printing substrate. The other approach for fabricating a TFT device is to utilize the paper substrate as a bifunctional material for both mechanical support and as a dielectric material.<sup>6</sup> The excellent porosity of paper will allow ion transport. This device architecture allows all-printed transistors to take full advantage of paper as an excellent printing substrate with a porous morphology. A wide range of other electronic devices have been demonstrated as well, including organic light-emitting diodes,<sup>7</sup> electronic memories,<sup>8</sup> actuators,<sup>9</sup> displays,<sup>10</sup> RFIDs,<sup>11</sup> and sensors. Recently, Osterbacka and Tobjork published an excellent review about paper electronics.<sup>2</sup>

Along with paper electronics, wearable electronics are attractive for many applications, such as consumer products, sport clothing, military, *etc.*<sup>12</sup> These niche applications would require the integration of functional devices into textiles or fabrics (Fig. 1 (c)).<sup>13</sup> These integrated electronic devices need to be flexible, light-weight and durable. Currently, most of the effort on wearable electronics is focused on the attachment of electronic devices onto the textile surface.<sup>14</sup> However, such detachable devices still need to be flexible. The idea of wearable electronics, or smart fabric, will require the fabrication of devices directly into the fabric. However, similarly to paper electronics, the rough surfaces of textiles makes this task extremely challenging. Recently, quite a few research groups have been working on electronic and sensing devices on textiles, including the Hines-troza group at Cornell University, Bucheley group at Massachusetts Institute of Technology and others.

### 1.3 Energy and environmental technologies for paper and textiles

The intrinsic rough surfaces of paper and textiles are problematic for electronic device fabrication. However, this property is ideal for many energy devices in which large surface roughness is actually preferred. Supercapacitors and Li-ion batteries, for example, share similar device structures, in which the surface roughness of the electrode, or current collector, is beneficial for manipulation of electrons and ions. In charging a Li-ion battery,

the electrons will move from the charger to the negative electrode, and the positive Li ion is transported from the positive electrode and across the separator to meet the negative electrons. Once the electron meets the ion, the charging process for this particular site is finished. Therefore, the manipulation of the electron and ion transport across the entire structure, especially inside the electrode, is crucial for the best utilization of electrode materials and for achieving high-power performance.

The surface roughness and the porous structure of paper and textile will be ideal for such manipulation, especially for ions. However, paper and textile substrates are not electrically conductive for electrons. The diameters of fibers in paper and textile are  $\sim 20\ \mu\text{m}$ , 20 000 times the diameter of nanoscale materials, such as single-walled carbon nanotubes (SWNTs). Our group has demonstrated that conformal coating of SWNTs on the surface of paper and textiles can instantly turn the paper or textile into a highly conductive medium for electron transport.<sup>15,16</sup> Similarly, conductive fabric or paper has been demonstrated by others as well.<sup>17,18</sup>

From this perspective, we will mainly summarize our own research on the demonstrations of various energy and environmental devices for conductive paper and textiles. Here, conductive paper and textiles refer to paper and textiles with a thin coating layer of SWNTs coating on the fiber surface, although we recognize that other conducting nanomaterials can be used as well. Note that in this article, paper and textiles broadly refer to a large range of choices (woven, non-woven, with different thickness and different materials such as cellulose and polyester). These devices fully benefit from the properties of paper and textiles: earth-abundant, porous, and roll-to-roll printable. These devices are fabricated using an extremely simple method and show outstanding device performances. The combination of nanotechnology and traditional paper and textile materials shows promise to provide high performance and low-cost solutions for addressing the enormous energy and environmental challenges.

## 2. Novel conductor based on paper and textiles

The properties of paper and textiles have been explored and well understood, and detailed documentation is available.<sup>19</sup> It is

worthwhile to summarize those closely related to applications in energy and the environment. Typically, a piece of paper has a thickness of  $\sim 20\text{--}200\ \mu\text{m}$ , and a textile has a thickness up to a few mm. In this article, we consider paper as a thin, flexible, 2D porous medium, and thick textiles as 3D media. One of the most amazing aspects is their morphology. Fig. 2 shows the surface morphologies of paper and textiles imaged with a scanning electron microscope (SEM). The surface of the paper is overcoated with 5 nm of gold for imaging purposes. The paper is made of randomly distributed cellulose fibers which have diameters of approximately  $20\ \mu\text{m}$ . The surface of each individual fiber is examined (Fig. 2(b)). Clearly, an individual fiber is made of thousands of smaller cellulose fibers, or nanocellulose (NFC). Note that the surface of the fiber is overcoated with gold only in this case, and the fibers do not have SWNTs. The surface area of a paper fiber has been measured to be  $\sim 230\ \text{m}^2\ \text{g}^{-1}$ .<sup>20</sup> The surface of paper is full of OH groups. The functional groups, porosity, and hierarchical structure of paper make it an excellent medium for printing, writing and light-weight packaging. For energy devices in which the manipulation of ions and charges is crucial, this porous structure will be extremely beneficial for achieving outstanding device performance. Indeed, there are thousands of types of paper, and their surface morphologies and porosities will highly depend on the material, the fabrication process (drying, pressing *etc.*), and post-treatment (polishing, whitening *etc.*), which offers a large number of options tailored towards specific energy and environmental technologies.

It is interesting to find out that many other materials have a similar porous, fibrous structure, including wood, grass, rags, cotton, wool, bamboo, *etc.* Fig. 2(c) and (d) shows a photograph and an SEM image of a textile. The surface of the textile is even more porous than paper, as shown in Fig. 2(a), which is beneficial for many applications as shown later. The material is polyester

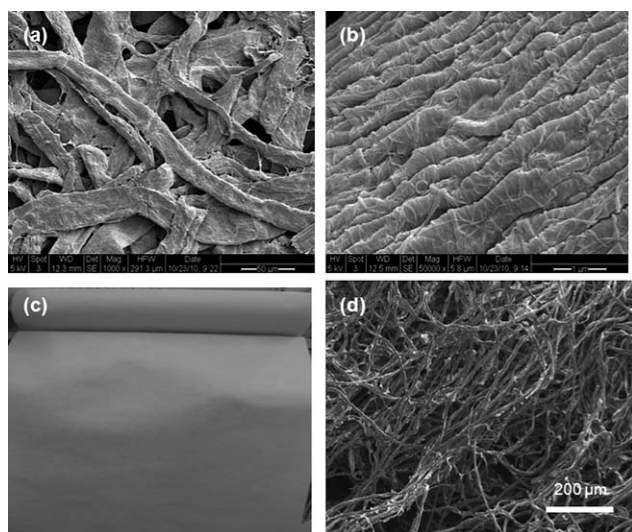


**Fig. 2** (a) A SEM image of paper surface with randomly distributed cellulose fibers. The diameter of a cellulose fiber is approximately  $20\ \mu\text{m}$ . (b) A high-resolution SEM image of a cellulose fiber surface. The cellulose fiber is coated with Au for imaging. (c) A photograph of a polyester textile roll from Walmart with a width of one meter and a thickness of  $\sim 5\ \text{mm}$ . The cost of such textile is  $\sim 1\ \$\ \text{m}^{-2}$ . (d) A SEM image of a textile surface in (c).<sup>15,16</sup>

and the textile is cheap,  $\sim 1\ \$\ \text{m}^{-2}$  from Walmart. The textile is resistant to high temperatures (up to  $200\text{--}300\ ^\circ\text{C}$ ), water, and many solvents. In this article, mainly non-woven textiles are used due to their better porosities for high-performance device applications.

One obvious method to make paper conductive is to deposit a thin layer of metal on its surface. Due to the large surface roughness of paper, the metal layer needs to be thick enough ( $\sim 50\ \text{nm}$ ) to obtain decent conductance. The metal coating will block the nanopores on paper fibers, which will make it hard for the deposition of subsequent layers through printing. In our recent studies, we fabricate highly conductive paper by a solution-based printing method.<sup>15</sup> Highly conductive, nanoscale, carbon-based nanomaterials, such as SWNTs and graphene, are used.<sup>21</sup> To fully take advantage of paper as an excellent printing substrate, solution-based deposition is used. Nanoink based on SWNTs and graphene has been studied extensively and is well understood. To form a SWNT ink, SWNT powder and sodium dodecylbenzenesulfonate (SDBS) were dispersed in deionized water, with concentrations of 10 and  $1\text{--}5\ \text{mg}\ \text{mL}^{-1}$ , respectively. After bath-sonication for 5 min, the SWNT dispersion was probe-sonicated for 30 min at 200 W to form a nanoink. The nanoink is stable at room temperature for at least one week (Fig. 3(a)). Due to the porous structure of paper, the contact angle of nanoink on paper is much smaller than that on a plastic substrate (Fig. 3(b) and (c)). In the field of printing electronics on plastics, significant efforts have been spent on the ink formulation and the rheology adjustment.<sup>22</sup> The goals include: (1) matching the surface energy between the substrate and the ink, (2) making the ink viscosity high enough to be resistant to turbulence during the drying process, (3) controlling the drying dynamics and temperature gradient for uniform drying, (4) washing of surfactant, and (5) ensuring the finished film has enough binding energy to the substrate to survive the washing process. Polymer binders or adhesive layers are used to enhance the binding energy. Additives are typically needed to adjust the ink properties, which will increase the complexity of the nanoinks and results in high cost and low throughput fabrication on plastic substrates.<sup>23</sup> In sharp contrast, printing on paper substrates will have many fewer requirements for the nanoink. Different fabrication methods have been applied for fabricating conductive paper, and Chinese calligraphy and pen writing were demonstrated as examples (Fig. 3(d)). The SWNT nanoink also can be ink-jet printed on paper substrates in patterns, which is significant because many devices would need conductive pads (Fig. 3(e)). Direct printing with an ink-jet printer is a material-saving, high-speed, and low cost process. For use as current collectors for supercapacitors or Li-ion battery applications, continuous nano-films are needed. A scalable Meyer rod coating method was applied. The SWNT ink was applied to the paper surface, and a Meyer rod, which provides thickness control, was rolled over the ink. Instantly, the paper was transformed into highly conductive paper with a low sheet resistance of  $\sim 1\text{--}10\ \text{Ohm}\ \text{sq}^{-1}$ . The instant coating and drying is due to the porous structure of paper, which can absorb the solvent quickly. Capillary forces also enable the large contact area between SWNTs and paper fibers.

Conductive paper fabricated with methods in Fig. 3 has excellent properties, which were discussed in detail elsewhere.<sup>15</sup> Due to the size difference of SWNTs and fibers and their strong binding

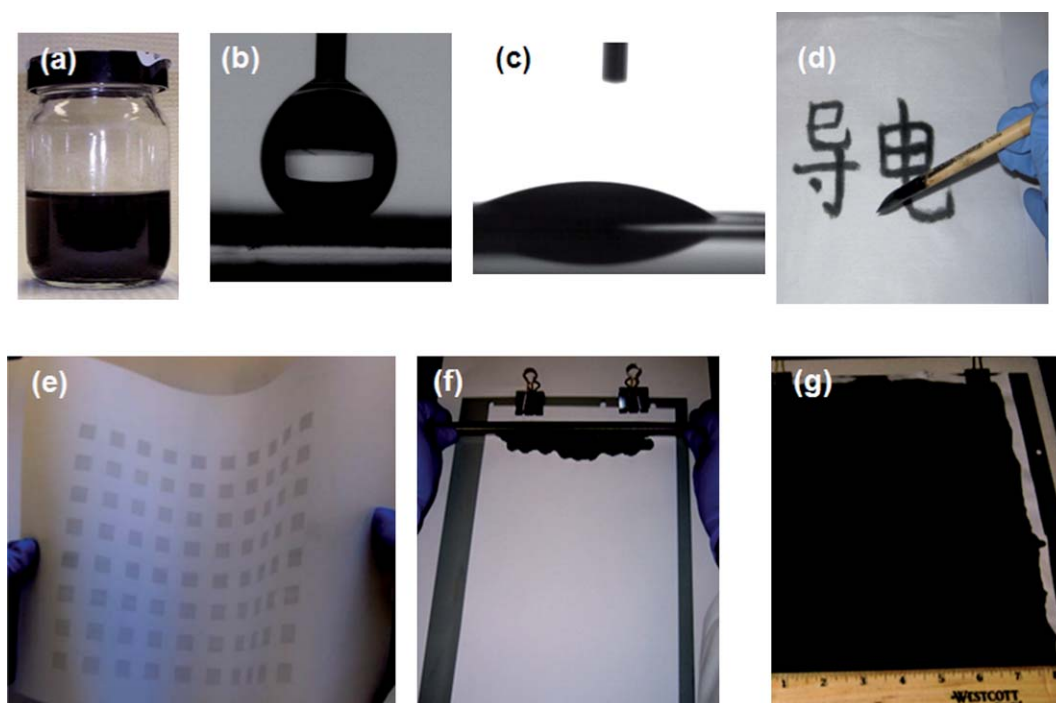


**Fig. 3** (a) Stable ink with well-dispersed SWNTs in water with a concentration of  $1 \text{ mg mL}^{-1}$ . (b) and (c) Contact angle for SWNT ink on plastic PET and paper substrate, respectively. The paper substrate shows much better wetting with SWNT ink than the plastic substrate. (d) Direct writing of SWNT ink on the paper with Chinese calligraphy. (e) A photo of ink-jet printed SWNT patterns on both sides of the paper. (f) Meyer rod coating of CNT or Ag NW ink on commercial Xerox paper. (g) Conductive Xerox paper after CNT coating with sheet resistance of  $10 \text{ Ohm sq}^{-1}$ .<sup>15,24</sup>

force, SWNTs can wrap around fibers to make individual fibers highly conductive (Fig. 4(a)).<sup>16</sup> Fig. 4(b) and (c) show the surface morphology of conductive paper with a sheet resistance of  $10 \text{ Ohm sq}^{-1}$ . The highly porous structure of pristine paper is maintained, as the thickness of the SWNT coating is much less than that of the paper fiber diameter. Paper and textiles have macroporous structures, and a SWNT film has a microporous structure. This is called a double porous structure in this article.

It is well understood that SWNTs have excellent mechanical flexibilities due to their large aspect ratios. Meanwhile, the large capillary force during the drying process for nanoink will maximize the contact area between the SWNTs and the paper fiber, increasing the van der Waals forces between the SWNTs and paper. Therefore, an excellent conformal coating was observed, as shown in Fig. 4(c). As a result, the conductive paper is highly flexible and can be bent down to a radius of 2 mm and even folded without a change in sheet resistance (Fig. 4(d)). We also applied the same method to produce conductive paper based on other types of nanoinks, such as silver nanowires (Ag NWs) in methanol. The sheet resistance at different effective film thickness for SWNTs and Ag NWs are plotted in Fig. 4(e). As the film thickness increases, the scaling of the resistance *vs.* thickness changes from percolation-like behavior to linear behavior. Other types of conductive paper have also been reported.<sup>25–27</sup> Here, we used widely available commercial paper, not paper-like films produced by much more complicated processes. The goal is not only to benefit from the unique properties of paper to achieve outstanding performance in devices, but also to lower the cost of energy devices by utilizing existing materials and manufacturing infrastructure.

As discussed earlier, textiles are also made of fibers which have diameters of  $\sim 20 \mu\text{m}$ . These fibers have a hierarchical structure with a novel surface morphology and different functional groups. Compared to paper, textiles are much thicker and more porous, which are crucial for some applications.<sup>13</sup> As textiles can absorb much more solvent, and do it more quickly, we apply the dipping-drying method to fabricate conductive textiles, which is very similar to the dyeing process in the traditional textile industry. As shown in Fig. 4(a), a textile can instantly absorb enough SWNT ink and change from white to black in less than a second. Such a quick process will be important when roll-to-roll large-scale manufacturing is needed for industrial applications. After drying, the conductive textile shows excellent properties. The details can be found in our previous publication.<sup>16</sup> Fig. 5(b) and (c) show the SEM images of individual textile fibers coated with SWNTs on the surface. The thickness of the CNT coating is approximately 200 nm. The resistance, as measured by a four probe measurement, is 600 Ohm for a fiber with a diameter of  $20 \mu\text{m}$  and length of 1 mm. Therefore the SWNT film conductivity is approximately  $1300 \text{ S cm}^{-1}$ , which is similar to the conductivity of SWNT films on plastic substrates. Similar to conductive paper, conductive textiles have excellent mechanical flexibilities, show excellent adhesion between SWNTs and the textile, and are resistant to various solvents (Fig. 4(d)–(f)). Note that conductive paper or conductive textiles in this article refers to paper and textiles overcoated with SWNTs. Previously conductive paper, textiles or fabric have been demonstrated by others. Gruner *et al.* demonstrate conductive, woven fabric with SWNTs, and the applications are mainly for electronics.<sup>17</sup> Varahramya *et al.* have demonstrated conductive fibers with layer-by-layer conductive polymer coating.<sup>28</sup> Wallace

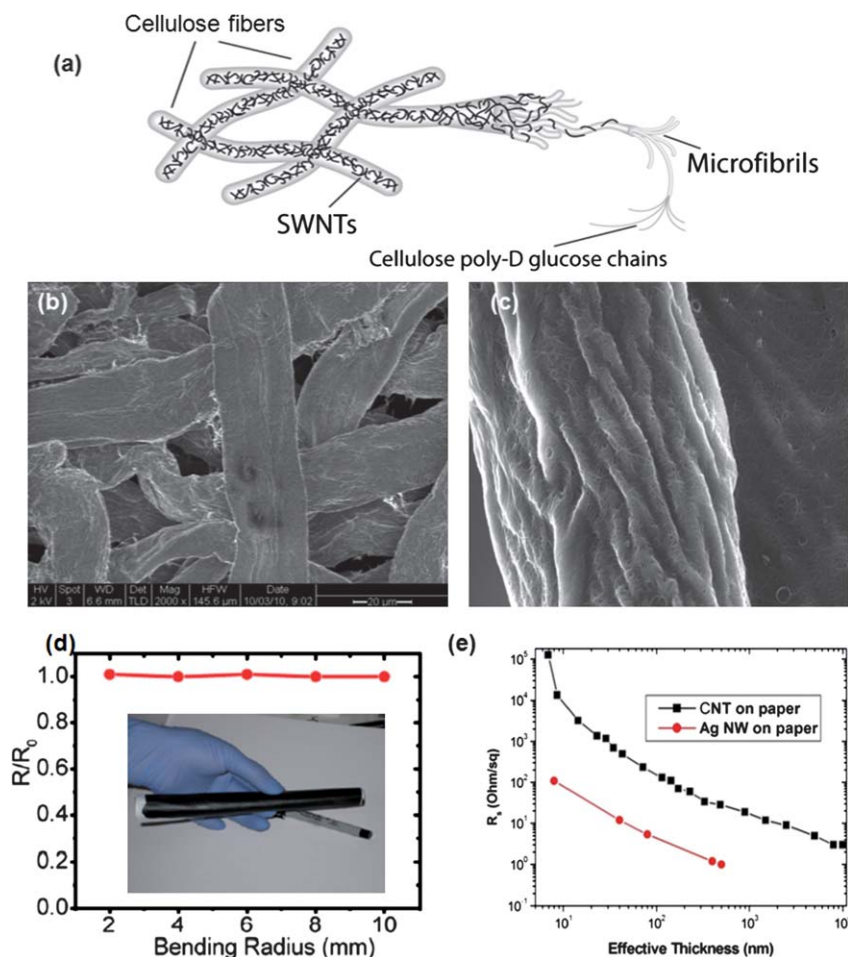


**Fig. 4** (a) Schematic of SWNTs wrapping around cellulose fibers to form a 3D porous structure. (b) SEM image of conductive paper with SWNT coating. The SWNTs conformally coat on the surface and bridge over the gaps between paper fibers. (c) An SEM image to show the excellent conformal coating of SWNTs due to their flexibilities and strong binding with paper fibers. (d) Sheet resistance changes after bending conductive paper into different radii. Inset shows that conductive paper is mechanically flexible. (e) Sheet resistances of conductive paper based on SWNTs and Ag NWs with various thicknesses.<sup>15</sup>

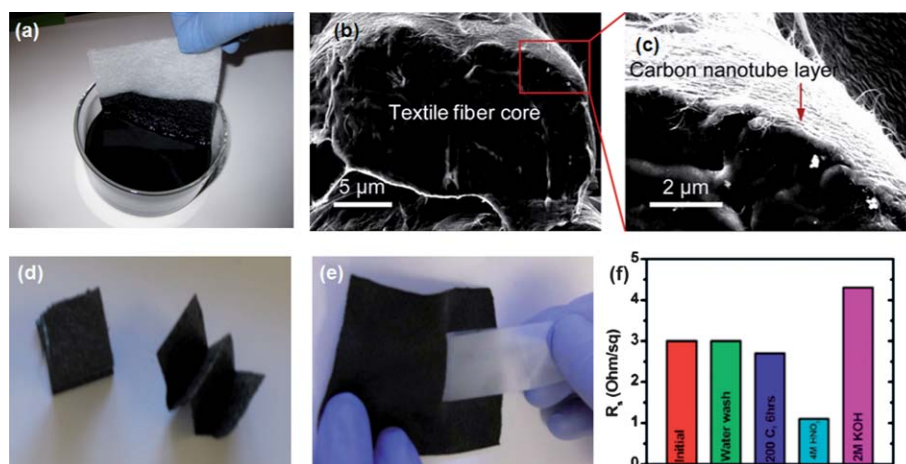


**Fig. 5** (a) A simple dyeing process for fabricating conductive textiles. A piece of white polyester textile is dipped into a black SWNT solution. (b) Cross section of textile fiber. (c) The interface between the SWNT layer and the textile fibers. The thickness of the SWNTs is 200 nm. (d) The conductive textile is extremely flexible. Even after being folded a few times, there is no notable change for the sheet resistance. (e) A scotch tape test shows the excellent binding between SWNTs and textile. (f) SWNT/textile is resistant to water washing, thermal treatment at 200 °C for 6 h, 4 M HNO<sub>3</sub> acid, and 2 M KOH.<sup>16</sup>

reported textile supercapacitors with incorporated conductive textiles.<sup>29</sup> Kotov *et al.* demonstrated a smart sensing device on a textile substrate with the use of SWNTs.<sup>30</sup> In this article, we will focus on conductive paper and textiles enabled by a solution-based printing or dyeing process for regular paper and textile substrates.

There are many remaining fundamental questions involving conductive paper and textiles, such as the exact binding energy between nanoscale materials and textile fibers, the adhesion force between the film and textile, the mechanism for automatically removing surfactant, the drying dynamics for nanoink on paper, the level of remaining surfactant on the surfaces of SWNTs, *etc.* Meanwhile, one can imagine incorporating other conductive nanoscale materials to fabricate conductive paper, such as graphene or metal nanostructures.<sup>21</sup> The other goal of this report is to investigate the device applications of conductive paper and textiles for energy and environmental devices. The major motivation is to replace the traditional conductor with these novel conductors (Fig. 6). For example, heavy metal foils such as copper and aluminum are widely used in Li-ion batteries. These metals are heavy and non-porous, but they have been used throughout history. On the other hand, porous carbon-based electrodes have been developed and used, such as carbon cloth as shown Fig. 6(c).<sup>31</sup> However, carbon cloth is not as porous as conductive textiles which will be discussed later. Carbon cloth refers to a range of carbon fibers carbonized from pitch, PAN or acrylic yarn.<sup>32</sup> The remaining sections will be devoted to the exploration of devices based on conductive paper and textiles. These few examples will only show the tip of the iceberg, leaving many topics to explore in the future.

### 3. Energy and environmental technologies for conductive paper and textiles: examples

#### 3.1 Flexible energy storage

Flexible electronics is emerging for consumer applications and attractive for some untraditional applications in which device mechanical flexibility is preferred or required. To fully realize

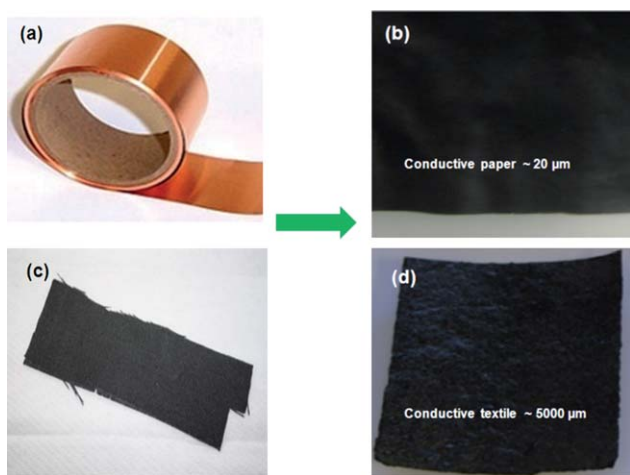


**Fig. 6** Shift from traditional conductors to new conductors based on paper and textiles. For thin conductors, conductive paper (b) replaces heavy metal foil, *i.e.* Cu foil (a). For 3D porous conductors, conductive textile (d) replaces carbon cloth (c).

flexible electronics, integrated flexible energy storage is needed. Recently, there have been quite a few nice publications about flexible energy harvesting and storage devices.<sup>33–37</sup> It has been found that the flexibilities of functional devices are largely determined by the flexibilities of the electrodes or current collectors. The typical failure mechanism is due to the conductors. For example, tin-doped indium oxide (ITO) is widely used as a transparent electrode for optoelectronics. However, the mechanical cracking and breaking of this layer is the main cause of the failure of the entire device.<sup>38</sup> Conductive paper and textiles are highly conductive and mechanically flexible, which can enable a range of flexible electronics to be built on it. To take advantage of the highly porous structure of the conductive paper, we have successfully demonstrated flexible energy devices on paper, in which conductive paper or textiles are used as essential components.

Due to their large surface areas, SWNTs have been explored as attractive supercapacitor materials using the electrochemical double layer mechanism.<sup>39–41</sup> Because of the high conductivity of the SWNT film on our conductive paper, we designed and demonstrated flexible supercapacitors based on conductive paper, on which SWNTs function as both the current collector and the electrode material.<sup>42</sup> The surfaces of SWNTs deposited on porous paper are highly accessible to ions in the electrolyte. Fig. 7(a) shows the structure of an all-paper supercapacitor, in which two pieces of conductive paper are used as the cathode and the anode, and another piece of plain paper is used as the separator.<sup>15</sup> In other work, we demonstrated that all the components can be integrated into a single sheet of paper through ink-jet printing. This all-paper based supercapacitor is ultrathin and highly flexible. Its performance in both aqueous and organic electrolytes has been tested using galvanostatic and cyclic voltammetric methods. Fig. 7(b) shows the voltage profile during charging and discharging for two different electrolytes. The IR drop is used to calculate the internal resistance of the device. Paper-based supercapacitors show much higher specific capacitances than devices based on plastic substrates (Fig. 7(c)). At a high current density of up to  $40 \text{ A g}^{-1}$ , a capacitance of  $\sim 70 \text{ F g}^{-1}$  was maintained. The specific capacitance at high rates is much higher than that on plastic substrates which lacks the porous structure. This is clearly due to the excellent ion transport of SWNTs on paper. We have carried out a control experiment in which conductive paper is fabricated by a thin layer of gold deposition. The same mass of SWNTs was deposited on the conductive paper as the electrode material. The specific capacitance of SWNTs is much worse because the gold coating blocks the pores in cellulose paper, which impedes the ion access from the paper fibers.

Based on the capacitance, impedance, current density and voltage, the energy density and power density are calculated with the mass of SWNTs (Fig. 7(d)). It is not surprising that the all-paper based supercapacitor shows much better performance. To compare with commercial supercapacitor performance, the total weight (including SWNTs, electrolyte, paper, separator) of the energy device, instead of the electrode material only, should be used in the calculation. As shown in Fig. 7(e)), the energy density and power density of the device is still much higher than commercial supercapacitors. Cycling life is one of the most critical parameters in supercapacitor operation. After careful

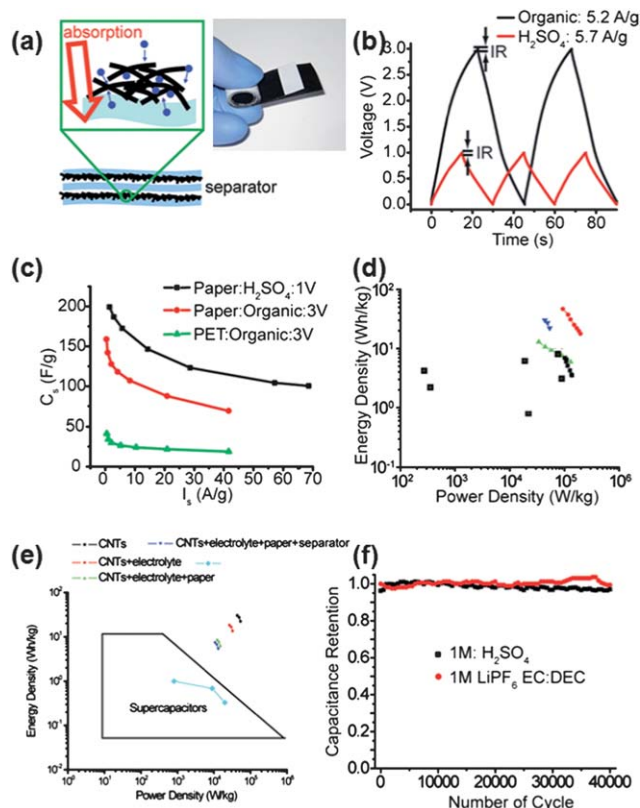


**Fig. 7** Flexible all-paper supercapacitor using conductive paper as the electrodes and current collectors. (a) Schematic drawing of the device structure. Zoomed-in schematic illustrates that ion accessibility is improved due to the porous structure of paper. A photograph of a real assembled device is also shown. (b) Galvanostatic charging and discharging curves with organic electrolyte and sulfuric acid. (c) Gravimetric capacitance and power density performances, which are based on the mass of SWNTs. (d) A Ragone plot showing the energy density and power density performances, which are based on the mass of SWNTs. (e) A Ragone plot showing the densities with different combinations of dead components. (f) Capacitance retention measured in different electrolyte. After 40 000 cycles, 97% and 99.4% of initial capacitance is maintained for sulfuric acid and organic electrolytes, respectively.<sup>15</sup>

sealing, the supercapacitor based on conductive paper demonstrated excellent cycling performance, as shown in Fig. 7(f).

Compared to supercapacitors, Li-ion batteries have much higher energy densities with respect to the weight and the volume of the devices. Flexible Li-ion batteries with conductive paper as the current collectors for both the anode and cathode have been demonstrated as well. Fig. 8(a) shows the device structure of the conductive paper based Li-ion battery, in which the battery electrode materials ( $\text{LiMn}_2\text{O}_4$  nanorod as cathode and  $\text{Li}_4\text{Ti}_5\text{O}_{12}$  particle as anode) were coated on the surface of conductive paper with a slurry process. The half cells were tested with Li-metal as the counter electrode. The voltage profiles of both electrodes are consistent with the literature (Fig. 8(b)).<sup>43,44</sup> No apparent voltage drop was observed. A full cell with conductive paper as both current collectors was also demonstrated (Fig. 8(c)). The conductive paper based Li-ion battery also shows excellent cycling performance (Fig. 8(d)). The capacity retention was 95% after 280 cycles at a rate of C/3. During the following 220 cycles at a rate of C/2, less than 0.01% capacity is lost per cycle. The cell

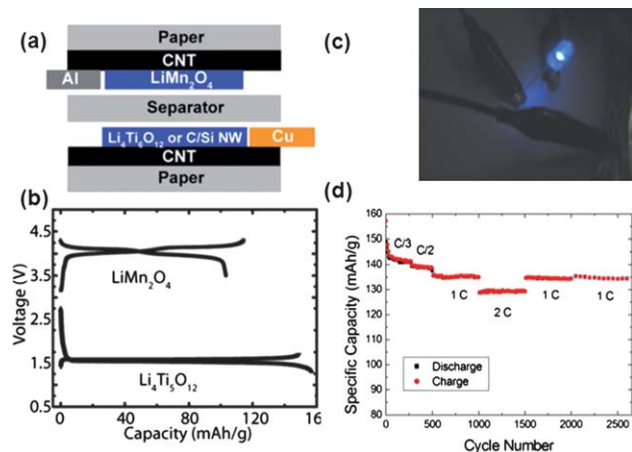


**Fig. 8** Conductive paper as the current collector for Li-ion batteries. (a) A schematic illustration of the device structure in which conductive paper is used as the current collector for both the anode and cathode. (b) Galvanostatic charging and discharging curves of  $\text{LiMn}_2\text{O}_4$  nanorod cathode (3.5–4.3 V) and  $\text{Li}_4\text{Ti}_5\text{O}_{12}$  nano-powder anode (1.3–1.7 V) half cells with conductive paper as the current collectors. (c) A 5 cm<sup>2</sup> paper battery lighting up a LED device. (d) Cycling performance of half cells with different C rates. 1 C is charging and discharging in 1 h each and 2 C is charging and discharging in 0.5 h.<sup>15</sup>

was still functioning after cycling for 9 months continuously. These experiments confirm that conductive paper is extremely stable in the electrolyte and the voltage range, and the adhesion between the electrode and the conductive paper is excellent.

By using a totally different process, a fully-integrated flexible Li-ion paper battery was recently demonstrated.<sup>45</sup> As shown in Fig. 9(a), highly conductive SWNT films were used as current collectors for both the anode and cathode. The Li-ion battery materials were coated on the surface of SWNT films and the double-layer films were delaminated from the metal substrate due to poor adhesion between SWNTs and metal.<sup>45</sup> Such

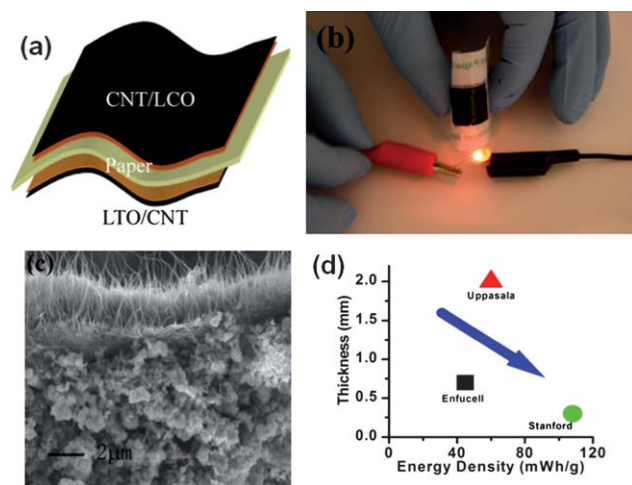


**Fig. 9** Integrated thin, flexible Li-ion paper battery. (a) Schematic of the final paper Li-ion battery device structure. The paper is used as both the separator and the mechanical support. (b) Picture of a highly flexible Li-ion battery lighting up a LED device. (c) SEM image of the cross section of SWNT/LTO double layer. (d) Comparison of our paper Li-ion battery with other flexible energy storage devices.<sup>45</sup>

free-standing films with integrated current collectors and electrode materials were laminated onto the paper surface. Fig. 9(b) shows a highly flexible, rechargeable paper battery lighting up an LED device. The interface between the SWNT film and the electrode material can be easily identified (Fig. 9(c)). Highly porous paper functions as both the mechanical support and the separator membrane. From an impedance measurement, it is found that the paper substrate has a smaller  $I/f$  ratio, where  $I$  is the tortuosity and  $f$  is the pore fraction. The total impedance of the electrolyte across a porous separator is  $R = (I/f) \cdot (\rho L/A)$ , where  $\rho$  is the electrolyte resistivity,  $L$  is the distance and  $A$  is the separator area.  $I/f$  is 9.1 for paper and is 28.8 for a standard separator membrane. The Li-ion paper battery also shows excellent cycling and self-discharge performance, which indicates that the paper separator has an outstanding electrochemical performance in the voltage range. For thin, flexible energy device applications, the energy density and the total thickness are important parameters. Fig. 9(d) shows the comparison of our paper device with other commercial thin, flexible energy storage devices.

### 3.2 Stretchable and wearable textile supercapacitors

Stretchable electronics is another emerging area that is expected to enable a range of new applications. Many functional devices have been demonstrated, such as stretchable transistors and displays.<sup>46,47</sup> For fully integrated stretchable electronics, stretchable power devices are needed. Just as with flexible electronics, the electrode is always the limiting factor for new types of electronics. Stretchable electrodes or conductors have been demonstrated, mainly based on one-dimensional (1D) materials such as SWNTs and nanowires. Upon stretching, these 1D materials can bridge the gaps to maintain a percolative conduction path.<sup>48</sup> Recently, a stretchable electrode based on graphene and porous PDMS has been demonstrated. It is well-known that most fabric is stretchable, which is a basic function for clothing. Fig. 10(a) shows the surface morphology of a stretchable, woven fabric, in which the fibers are interlocking. Such fabric can be stretched more than 2.4 times its initial length. When SWNTs are conformally coated on the surface of the fibers, the fabric becomes highly conductive with a sheet resistance of  $\sim 10 \text{ Ohm sq}^{-1}$ . To test the elasticity, the resistance of the conductive fabric is monitored as it is being loaded in a tensile tester. It is amazing that the resistance decreases as the fabric is stretched (Fig. 10(b)). This phenomenon is due to the improvement of the electrical contact between the textile fibers. As the fabric is stretched further, the fibers become damaged and the electrical contact resistance between fibers increases. Using the stretchable conductors, stretchable supercapacitors are fabricated with stretchable textiles as the electrodes and another plain textile as the separator. This integrated, full-textile supercapacitor (Fig. 10(c)) is highly stretchable and shows excellent capacitance retention after being stretched to 120% strain for 100 cycles (Fig. 10(d)). The conformal SWNT coating functions as both the supercapacitor active material and the current collector.

### 3.3 Three-dimensional energy storage devices

Both a supercapacitor and a Li-ion battery consist of multiple components, including the separator, anode, cathode, current

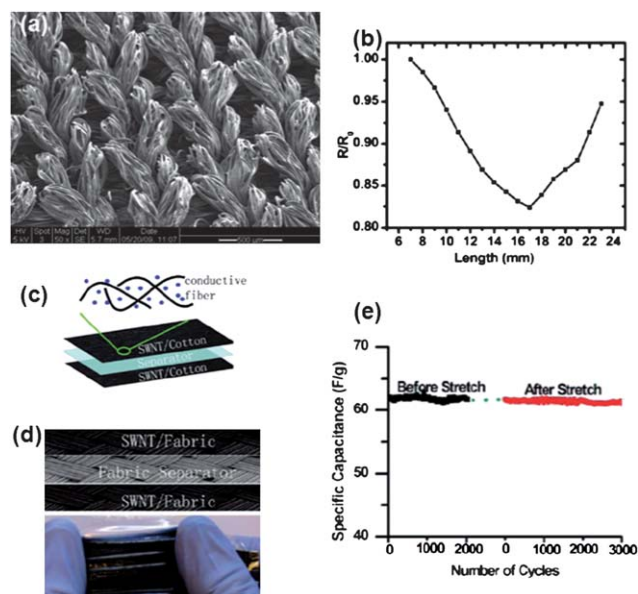


**Fig. 10** All-textile stretchable supercapacitor. (a) SEM image of fabric sheet coated with SWNTs on the fabric fiber surface. The fabric fibers are interwoven together. (b) The SWNT-coated fabric shows unusual stretching properties. The film sheet resistance decreases as the SWNT/fabric is stretched up to 240% of its initial length, after which the resistance starts to increase due to the damage of the fibers. (c) Supercapacitor structure with porous textile conductor as electrodes and current collectors. (d) All-textile supercapacitor under stretching. (e) The specific capacity for a stretchable supercapacitor before and after stretching to 120% strain for 100 cycles with a current density of  $1 \text{ mA cm}^{-2}$ .<sup>16</sup>

collectors, electrolyte, and packaging. In order to improve the energy density and the power density with respect to the total weight or the total volume of the devices, the weight or volume percentage of the active electrode materials, which increases with the electrode thickness, is important. Typically, the electrode materials or composites are coated on flat metal substrates. This electrode is conductive for electrons and ions. As the electrode thickness increases, the impedance associated with the ion or electron transport also increase dramatically, leading to a large internal resistance and overpotential, which is detrimental to the device efficiency and stability performance. Thick ( $\sim 5 \text{ mm}$ ), macroporous conductive textiles provide an excellent conductive backbone for constructing three-dimensional (3D) energy storage systems. The electrode materials for supercapacitors, Li-ion batteries or other energy systems can be loaded directly into the pores of the conductive textile through solution-based processes, or overcoated on the surface of the conductive textile fibers through electrodeposition. Such textiles have universal structures, and this method can be applied to any sort of electrode material. The electrochemical stability of conductive textile has been found to be stable up to 3.8 V. Conductive textile is also chemically compatible with the traditional battery slurry process, involving *N*-methylpyrrolidone (NMP) and baking up to  $100^\circ \text{C}$ .

Fig. 11(a) and (b) show the scheme of a supercapacitor electrode design on a flat metal substrate and some porous conductive textile fibers with  $\text{MnO}_2$ .<sup>49</sup> While  $\text{MnO}_2$  is a promising material for supercapacitor applications due to its high specific capacitance and low cost,  $\text{MnO}_2$  suffers from low

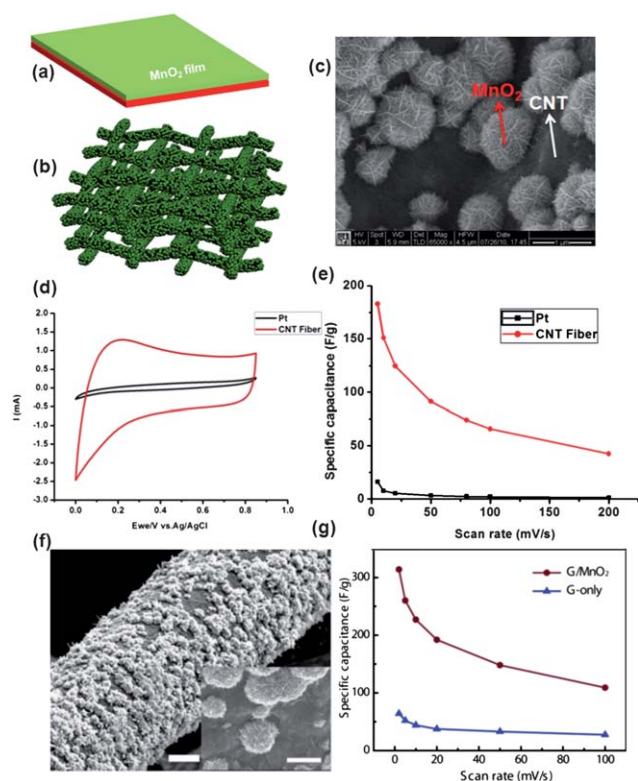


**Fig. 11** Nanostructured  $\text{MnO}_2$  supercapacitor based on conductive textile. (a)  $\text{MnO}_2$  films on metal film. (b)  $\text{MnO}_2$  films on conductive textile fibers. With the same mass loading, the thickness of  $\text{MnO}_2$  on textile fibers is much less than that of the metal film. (c) SEM image of  $\text{MnO}_2$  decorated on conductive textile. The interface between  $\text{MnO}_2$  nanoparticles and the CNT surface is clearly observed. (d) Cyclic voltammety test for (a) and (b), in which  $\text{MnO}_2$  mass densities ( $1 \text{ mg cm}^{-2}$ ) are the same for the Pt film and conductive textile. (e) The comparison of the specific capacitance. (f) SEM image showing the  $\text{MnO}_2$  nanoparticles and a clear interface between  $\text{MnO}_2$  nanoflower and graphene nanosheets underneath. Scale bars are 5 and 1  $\mu\text{m}$  for the main figure and inset, respectively. (g) Comparison of specific capacitance values between graphene/ $\text{MnO}_2$  textile and graphene nanosheets-only textile at different scan rates.<sup>21,50</sup>

electrical and ionic conductivities. As shown in Fig. 11(a) and (b), the thickness of  $\text{MnO}_2$  on the textile fiber surface is much less than the thickness of  $\text{MnO}_2$  on the flat metal substrate, if the total mass of  $\text{MnO}_2$  per projected area is the same. The decreased thickness will significantly improve the transport for both electrons and ions, which will help achieve high supercapacitor performance. The  $\text{MnO}_2$  was electrodeposited on the conductive textile by a scalable process.  $\text{MnO}_2$ , SWNT and textile substrate can be easily identified in Fig. 11(c). Detailed data are well documented and will only be briefly summarized.<sup>49</sup> Fig. 11(d) and (e) show the CV comparison between devices shown in Fig. 11(a) and (b), at scan rates of  $5 \text{ mV s}^{-1}$  and  $50 \text{ mV s}^{-1}$ , respectively. With the same mass loading of  $1 \text{ mg cm}^{-2}$ , the capacitance for the conductive textile based device is much higher than that of the metal substrate. As shown in Fig. 11(e), a specific capacitance of  $370 \text{ F g}^{-1}$  is achieved for the conductive textile-based device, while only  $36 \text{ F g}^{-1}$  for the metal-based device. This 10-fold difference in specific capacitance respective

to the mass of  $\text{MnO}_2$  at the same scan rate must be due to the kinetics of ions and electrons inside the electrode materials.

Another scalable method to fabricate energy textiles is using the slurry-based dyeing process. An energy slurry typically includes electrode materials for batteries or supercapacitors, conductive additives, such as conductive carbon nanoparticles, polymer binder, and organic solvent such as NMP. As shown in Fig. 12(a), an integrated electrode–current collector structure can be easily formed through the simple dyeing–drying process.<sup>49</sup> The conductive textile reduces in thickness dramatically when it is dried. The final thickness of the energy textile with embedded electrode materials is typically  $\sim 680 \mu\text{m}$  with a mass density of  $\sim 170 \text{ mg cm}^{-2}$ . The mass density is 8–10 times higher than that of metal current collectors. Conductive textile with SWNT overcoating, Super-P conductive carbon and battery material ( $\text{LiFePO}_4$ ) in this study can be easily identified by SEM (Fig. 12 (b)). In such an electrode, the charge transport is along the conductive textile fiber globally and along Super-P locally. This unique conduction path greatly enhances the charge transport in the electrode. Meanwhile, as mentioned above, conductive textile fibers absorb electrolyte and can maximize the accessibility of the ions to the electrode materials, which decreases the impedance associated with ion transport. The excellent transport for ions

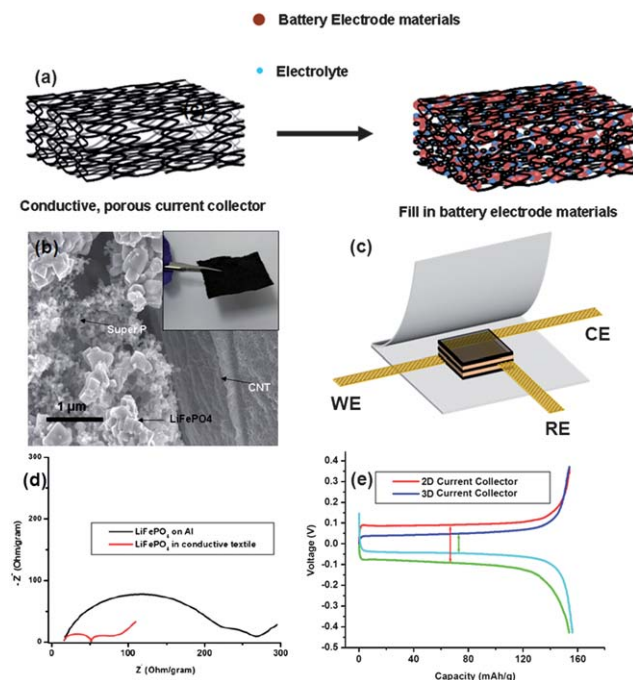


**Fig. 12** 3D Li-ion battery with conductive textile. (a) Design and fabrication of 3D porous current collectors filled with the battery electrode materials through a simple dipping–drying process. (b) SEM shows the interface between  $\text{LiFePO}_4$ , conductive additive and conductive polyester fibers coated with SWNTs. Inset shows a solid textile filled with battery materials. (c) A scheme of a three-electrode cell, where CE = counter electrode, WE = working electrode and RE = reference electrode. (d) Impedance spectra normalized by the weight of  $\text{LiFePO}_4$  where the 3D electrode shows a much smaller impedance. (e) Voltage profile of  $\text{LiFePO}_4$  vs. the reference electrode in the three-electrode cell for both 3D and flat architectures, where the 3D electrode shows a much smaller overpotential.<sup>51</sup>

and electrons across the entire electrode structure leads to much better performance than the device with metal current collectors. Because the areal mass loading is large, the current density is high which will cause potential fluctuations on the Li-metal side during measurement. Therefore, a three-terminal measurement configuration is used, in which a porous, 50% charged  $\text{LiFePO}_4$  electrode is used as the reference (Fig. 12(c)). The  $\text{LiFePO}_4$  will have a flat voltage profile as a reference. The electrochemical performance was compared for batteries with two different current collectors (conductive textile vs. metal). Electrochemical impedance spectroscopy was used to identify the internal resistance of the device at different frequencies. As shown in Fig. 12(d), the middle frequency semicircle and the diffusion part are similar for the two collectors. However, the pore resistance calculated with equivalent circuit modeling is 768 Ohm mg for the metal collector and 6.95 Ohm mg for the textile collector. The textile conductor shows 100 times less pore resistance, which explains its much smaller overpotential (Fig. 12(e)). The overpotential for  $\text{LiFePO}_4$  on Al is  $\sim 0.1$  V, which is twice that of  $\text{LiFePO}_4$  embedded in the 3D textile current collector.

### 3.4 Energy from waste water using microbial fuel cells

A microbial fuel cell (MFC) using the catalytic activity of microorganisms to produce energy from waste water is an excellent interface between energy and environmental science. Fig. 13(a) shows the device structure and operation of a MFC, in which waste in water is consumed and energy is produced. Electrode designs are important for achieving excellent device performance. In a MFC, the electrodes need to have high conductivities, chemical stabilities, bio-compatibilities, resistances to decomposition, catalytic activities, high porosities, to allow internal colonization and have strong interactions with bio-films. Various commercially available carbon-based porous

electrodes have been used, such as carbon cloth, carbon paper, foam and carbon brush.<sup>32</sup> However, these carbon-based electrodes do not have the ideal size compatibility with microbial organisms, which is needed for maximizing the internal colonization. However, the conductive textile with polyester fibers has excellent size compatibility. We have demonstrated the outstanding device performance of conductive textile electrodes for both the cathode and anode.<sup>31,52</sup> Fig. 13(b) and (c) show SEM images of the microorganisms over the conductive textile. Details can be found in our recent publication.<sup>31</sup> The microorganisms can grow on the entire conductive textile, as well as deep inside the textile, which is due to the macroporous, open structure of the conductive textile. In contrast, microbial colonization was largely restricted to the outer surface of the carbon cloth (Fig. 13(d)), with few microorganisms present on the interior fibers. This is due to the poor size compatibility and poor substrate transport inside the carbon cloth. Assuming all of the surfaces of the SWNT–textile fibers are accessible, the anolyte–biofilm–anode interface area is 10-fold larger than the projected surface area of a standard anode.

Due to their double-scale porous structure, conductive textiles also have excellent interactions with the microbial biofilms. The reasons are: (1) the SWNT coating on the textile fibers has nanoscale porosity, which will provide more contact area than the smooth surface of carbon cloth fibers. This enhanced contact area could result in stronger mechanical binding and more efficient charge transfer between the cell membranes and the electrode; (2) the high surface area of the conductive textile with functional groups to collect electrons from electron mediators, or shuttles, in the electrolyte; (3) the SWNT layer interacts effectively with microbial nanowires; these nanowires were found to be able to bridge the gap between SWNTs and even penetrate the anode surface, enhancing the nanowires' functions as electron conductors. All of these are not possible for other non-nanoscale electrodes, such as carbon cloth or carbon paper. The excellent interaction between microorganisms and the conductive textile will improve the device performance with high power output and lower internal device resistance. The electrochemical impedance spectroscopy (EIS) data can help in understanding the charge transfer and the internal resistance inside MFCs. The diameter of the first semicircle in the EIS Nyquist curve (Fig. 14(a)) corresponds to the charge transfer resistance. The value is 30 Ohm for the MFC with a SWNT–textile anode and 300 Ohm for the MFC with a carbon cloth anode. The 10-fold improvement in charge transfer resistance confirms the superior performance of the SWNT–textile compared to the carbon cloth. Fig. 14(b) and (c) show the device performance, in which the values are normalized to the projected area of the anode. The maximum current density for the SWNT–textile was  $7.2 \text{ A m}^{-2}$ , which is 2.6 times that achieved by the carbon cloth anode. The maximum power density is  $1098 \text{ mV m}^{-2}$  for the MFC with a SWNT–textile anode and is  $655 \text{ mV m}^{-2}$  for that with a carbon cloth anode.

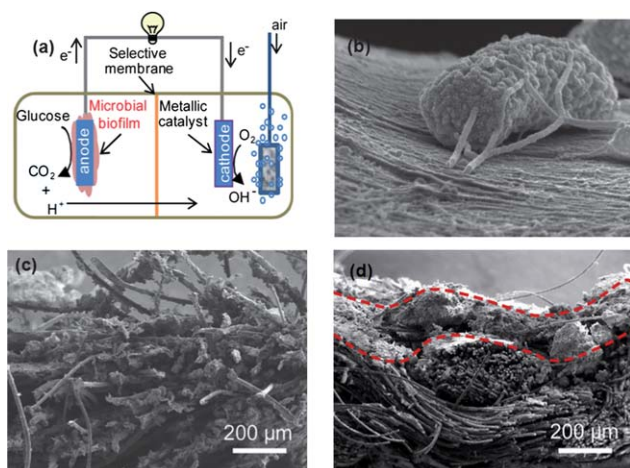


**Fig. 13** High performance microbial fuels using conductive textile as the anode. (a) A schematic of microbial fuel cells. (b) Microbial growth on conductive textile. (c) and (d) SEM cross sections to show the comparison of microbial growth on the conductive textile and carbon cloth, respectively. A microbial biofilm wraps around each SWNT–textile fiber, including both exterior and interior fibers. Due to the size compatibility, microbes can grow inside the conductive textile, while they only grow on the surface of the carbon cloth.<sup>31</sup>

### 3.5 Water sterilization based on conductive textile

Water sterilization is critical for many developing countries, in which a low-cost, high-throughput system is still lacking. Based on conductive textile, our group has designed and developed a totally new water sterilization device (Fig. 15(a)).<sup>53</sup> Unlike

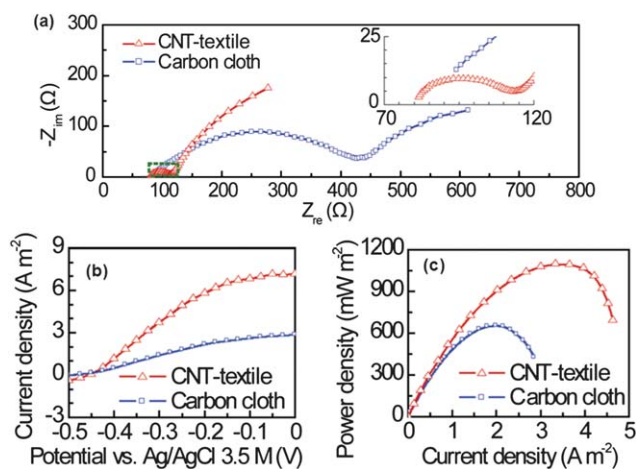


**Fig. 14** (a) Nyquist curve of the electrochemical impedance spectroscopy test for microbial fuel cells equipped with the conductive textile anode and the carbon cloth anode, respectively. The charge transfer resistance for conductive textile is 10 times smaller than that of carbon cloth (30 Ohm vs. 300 Ohm). (b) Linear stair voltammograms showing the maximum current density achieved on conductive textile is 2.6 times that achieved by the carbon cloth anode. (c) Polarization curve showing that the maximum power density of MFC prepared with conductive textile is 68% higher than that prepared with the carbon cloth.<sup>31</sup>

previous membrane-based methods, our conductive textile-based water filtration system does not rely on the size exclusion of bacteria, which requires a high pressure drop and suffers from frequent clogging and low energy efficiency. As shown in Fig. 15 (a), our design combines three components in different scales: SWNTs (diameter  $\sim 1$  nm), Ag NWs (diameter  $\sim 50$ – $100$  nm) and cotton fibers (diameter  $\sim 20\mu\text{m}$ ). The sheet resistance of the final conductive textile is approximately  $1 \text{ Ohm sq}^{-1}$ . The macroporous structure of cotton will allow dead bacteria to go through the conductive textile, avoiding the clogging problems. As contaminated water runs through the filter, a voltage is applied between the conductive textile and the copper wire in water. Fig. 15(b) shows the inactivation efficiency, defined as dead cell number/original cell number, vs. different applied voltage.

Ag NW/SWNT/cotton has much better performance than SWNT/cotton, which implies that the length at three different

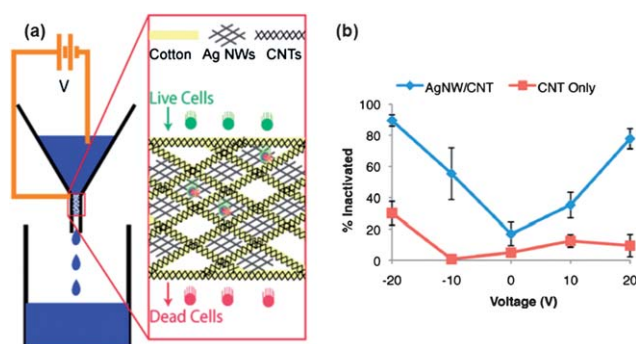


**Fig. 15** (a) Schematic of water filtration setup based on conductive cotton. A voltage is applied between the conductive textile and copper wire as water is filtering through the conductive textile. (b) Inactivation efficiency at different biases for AgNW/SWNT cotton as well as SWNT-only cotton.<sup>53</sup>

scales is important. At  $-20$  V, 89% of bacteria are inactivated. The filter size is 4 mm in diameter and 2.5 cm in length. The filtration process is running under gravity feed without the need for any applied pressure, which is more energy efficient than a membrane-based filtration system. When adjusted for filter size, a filtration speed of  $8000 \text{ L h}^{-1} \text{ m}^{-2}$  is achieved, much higher than typical membrane based systems ( $\sim 1 \text{ L h}^{-1} \text{ m}^{-2}$ ). The power consumption is also much less (only  $200 \text{ J L}^{-1}$  vs.  $\sim 1000 \text{ J L}^{-1}$ ). The mechanism can be: (1) silver or silver ions in solution; (2) the electrical field exceeding  $10^5 \text{ V cm}^{-1}$  at the nanoscale material surface affecting cell viability by breaking down the cell membrane.

The potential low cost of the material and fabrication process and the excellent device performance in terms of inactivation efficiency, energy efficiency and filtration speed make this technology an extremely attractive alternative as part of a future water purification system. There are concerns about the unanticipated health effects of nanomaterials in water, such as SWNTs and Ag NWs, especially SWNTs. Eventually SWNTs can be replaced with other nanoscale materials such as conductive polymers, or be totally removed. Although the efficiency will decrease, 87% bacteria inactivation can still be achieved with Ag NW/cotton systems (no SWNTs) in series. This study shows an excellent example application using new nanotechnology to address environmental and health challenges.

## 4. Summary

Regular paper and textiles can be turned into a highly conductive medium by overcoating a thin layer of SWNTs. These conductive paper and textiles are highly porous, flexible and even stretchable, and can serve as a novel conductors to replace traditional electrodes. Due to their novel double porous structure, high performance energy and environmental devices have been demonstrated, including flexible thin energy storage devices, stretchable supercapacitors, 3D energy textiles, microbial fuel cells using waste water, and high-speed water filtration devices. These energy and environmental devices can be fabricated with simpler processes and show superior performance compared to their counterparts with traditional conductors. In this article, SWNTs are mainly used as the model nanoscale materials. In terms of cost, SWNTs could be cheap with continuous development in manufacturing. The thickness of the SWNT coating is  $\sim 100$  nm, and the amount of material used for making conductive paper of textile is small. SWNTs share very similar properties (mechanical, chemical and environmental) with graphene and future development on using graphene in paper and textiles could be interesting. In addition, other conducting nanomaterials can also be explored to replace SWNTs. There are various kinds of paper and textiles, and we intentionally used low cost paper and textiles from Walmart. We could not give detailed comments on the cost of various paper/textiles, but we should be able to conclude that paper/textiles are lighter and cheaper than metal substrates which are currently used as current collectors for energy storage devices.

## 5. Research outlook

Paper and textiles are new substrates with very different morphologies than widely used substrates such as plastic, glass, or

metal for electronic devices. As excellent substrates for printing, fully integrated electronic devices on paper or textiles will not only allow macroelectronics with high-speed processing for low cost applications, but also enable a range of new applications that are not possible for other substrates. While paper or textile electronics, such as thin film transistors, RFID tags, and sensing devices have been developed before, they could benefit from the integration of the energy devices discussed in this study. Due to their unique double porous structure, conductive paper or textile based energy storage or environmental devices allow for fast transport of electrons and ions, which lead to the excellent performance of the energy devices. These devices are fabricated with an extremely simple dipping and drying process, which can be readily scaled up. Although SWNTs are expensive now, further development and commercialization will significantly decrease their cost. Other nanoscale conductive materials, such as multi-walled carbon nanotubes, graphene, metal nanostructures or conductive polymers can be used to replace SWNTs. These materials are believed to be cheaper than SWNTs. The low cost materials and high-speed solution-based process make conductive paper or textile based devices extremely promising for future applications. It is equally important that these energy devices have much better performance than those based on traditional conductors. In many cases, they even provide new functionalities that are not possible without the unique properties of paper or textiles. Meanwhile, there are a number of sustainable and recyclable paper/textiles that could be used for energy and environmental devices covered in this article. More detailed studies are needed to identify suitable materials which have the best properties such as porosity, interaction with nanoscale conductors, chemical and environmental stability, and cost for large-scale applications. Readers are encouraged to check further literature on the field of green and environmentally friendly materials for the same applications.<sup>54,55</sup>

Future research will help carry this new technology forward. Much fundamental understanding is still needed, such as the interaction between nanoscale materials and the macro-fibers, the transport of ions in the double porous electrode, the impedance of the 3D electrode, the interaction between the bio-nanowires and the conductive fibers, 2D vs. 3D comparisons for microbial fuel cells, etc. We only demonstrated a few applications of conductive paper or textiles, and many more applications should be explored in which new, porous conductors are needed. While individual devices are demonstrated, a system-level view should be taken, in which all the devices are integrated into a single sheet of paper or textile for fully-functional devices. Industrial efforts will help move this forward much faster. There are quite a few companies to commercialize paper and textile based devices with embedded electronics. Because roll-to-roll production is an old technology, large-scale energy or environmental devices should not be a problem using existing infrastructure. The union between nanoscale materials and paper or textile technology will open a wide range of new opportunities, which we believe will be far beyond what has been demonstrated in this paper.

## Acknowledgements

We acknowledge support from the King Abdullah University of Science and Technology (KAUST) Investigator Award (No.

KUS-I1-001-12). We also acknowledge Xing Xie, Mauro Pasta, Yuan Yang, David Schoen, Hui Wu, Fabio La Mantia, Jang Wook Choi, James R. McDonough, Sang Moo Jeong, Seung Min Han, Heather Deshazer, Benjamin Weil, Nian Liu, Wei Chen, Guihua Yu, Professor Craig S. Criddle and Professor Zhenan Bao.

## References

- 1 A. N. Nakagaito, M. Nogi and H. Yano, *MRS Bull.*, 2010, 35.
- 2 D. Tobjork and R. Osterbacka, *Adv. Mater.*, 2011, 23.
- 3 A. W. Martinez, S. T. Phillips and G. M. Whitesides, *Proc. Natl. Acad. Sci. U. S. A.*, 2008, **105**, 19606.
- 4 F. Eder, H. Klauk, M. Halik, U. Zschieschang, G. Schmid and C. Dehm, *Appl. Phys. Lett.*, 2004, **84**, 2673.
- 5 Y. H. Kim, D. G. Moon and J. I. Han, *IEEE Electron Device Lett.*, 2004, **25**, 702.
- 6 N. J. Kaihovirta, C. J. Wikman, T. Makela, C. E. Wilen and R. Osterbacka, *Adv. Mater.*, 2009, **21**, 2520.
- 7 V. L. Calil, C. Legnani, G. F. Moreira, C. Vilani, K. C. Teixeira, W. G. Quirino, R. Machado, C. A. Achete and M. Cremona, *Thin Solid Films*, 2009, **518**, 1419.
- 8 W. Lim, E. A. Douglas, S. H. Kim, D. P. Norton, S. J. Pearton, F. Ren, H. Shen and W. H. Chang, *Appl. Phys. Lett.*, 2009, 94.
- 9 J. Kim, S. Yun and Z. Ounaies, *Macromolecules*, 2006, **39**, 4202.
- 10 P. Andersson, D. Nilsson, P. O. Svensson, M. X. Chen, A. Malmstrom, T. Remonen, T. Kugler and M. Berggren, *Adv. Mater.*, 2002, **14**, 1460.
- 11 L. Yang, A. Rida, R. Vyas and M. M. Tentzeris, *IEEE Trans. Microwave Theory Tech.*, 2007, **55**, 2894.
- 12 X. Tao, *Wearable Electronics and Photonics*, 2006.
- 13 S. Park and S. Jayaraman, *MRS Bull.*, 2003.
- 14 M. B. Schubert and J. H. Werner, *Materials Today*, 2006, 9.
- 15 L. B. Hu, J. W. Choi, Y. Yang, S. Jeong, F. La Mantia, L. F. Cui and Y. Cui, *Proc. Natl. Acad. Sci. U. S. A.*, 2009, **106**, 21490.
- 16 L. B. Hu, M. Pasta, F. La Mantia, L. F. Cui, S. Jeong, H. D. Deshazer, J. W. Choi, S. M. Han and Y. Cui, *Nano Lett.*, 2010, **10**, 708.
- 17 D. S. Hecht, L. Hu and G. Gruner, *Curr. Appl. Phys.*, 2007, **7**, 60.
- 18 L. Wang, W. Chen, D. Xu, B. S. Shim, Y. Zhu, F. Sun, L. Liu, C. Peng, Z. Jin, C. Xu and N. A. Kotov, *Nano Lett.*, 2009, **9**, 4147.
- 19 M. Lewin and E. M. Pearce, *Handbook of fiber chemistry* Marcel Dekker Inc, New York, 1998.
- 20 J. E. Stone and A. M. Scallan, *J. Polym. Sci., Part C: Polym. Symp.*, 1965, 13.
- 21 G. Yu, L. Hu, Y. Cui and Z. Bao, *Nano Lett.*, 2011, **11**, 2905–2911.
- 22 L. B. Hu, D. S. Hecht and G. Gruner, *Chem. Rev.*, 2010, **110**, 5790.
- 23 A. A. Tracton, *Coating technology handbook* Marcel Dekker Inc, New York, 2000.
- 24 L. B. Hu, H. Wu and Y. Cui, *Appl. Phys. Lett.*, 2010, 96.
- 25 V. L. Pushparaj, M. M. Shaijumon, A. Kumar, S. Murugesan, L. Ci, R. Vajtai, R. J. Linhardt, O. Nalamasu and P. M. Ajayan, *Proc. Natl. Acad. Sci. U. S. A.*, 2007, **104**, 13574.
- 26 M. T. Byrne and Y. K. Gun'ko, *Adv. Mater.*, 1672, **22**.
- 27 P. Potschke, A. R. Bhattacharyya and A. Janke, *Carbon*, 2004, **42**, 965.
- 28 M. Agarwal, Y. Lvov and K. Varshney, *Nanotechnology*, 2006, **17**, 5319.
- 29 C. Y. Wang, A. M. Ballantyne, S. B. Hall, C. O. Too, D. L. Officer and G. G. Wallace, *J. Power Sources*, 2006, **156**, 610.
- 30 L. Wang, W. Chen, D. Xu, B. S. Shim, Y. Zhu, F. Sun, L. Liu, C. Peng, Z. Jin, C. Xu and N. A. Kotov, *Nano Lett.*, 2009, **9**, 4147.
- 31 X. Xie, L. B. Hu, M. Pasta, G. F. Wells, D. S. Kong, C. S. Criddle and Y. Cui, *Nano Lett.*, 2010, **11**, 291.
- 32 B. Logan, *Microbial Fuel Cells*, John Wiley & Sons, Inc, 2008.
- 33 Y. Qi and M. C. McAlpine, *Energy Environ. Sci.*, 2010, **3**, 1275.
- 34 H. Gwon, H.-S. Kim, K. U. Lee, D.-H. Seo, Y. C. Park, Y.-S. Lee, B. T. Ahn and K. Kang, *Energy Environ. Sci.*, 2011, **4**, 1277.
- 35 L. Nyholm, G. Nystrom, A. Mhramyan and M. Stromme, *Adv. Mater.*, 2011, **23**, 3751.
- 36 D. J. Lipomi and Z. Bao, *Energy Environ. Sci.*, 2011, **4**, 3314.
- 37 G. Wee, T. Salim, Y. M. Lam, S. G. Mhaisalkar and M. Srinivasan, *Energy Environ. Sci.*, 2011, **4**, 413.

- 38 D. S. Hecht, L. B. Hu and G. Irvin, *Adv. Mater.*, 2011, **23**, 1482.
- 39 C. M. Niu, E. K. Sichel, R. Hoch, D. Moy and H. Tennent, *Appl. Phys. Lett.*, 1997, **70**, 1480.
- 40 K. H. An, K. K. Jeon, J. K. Heo, S. C. Lim, D. J. Bae and Y. H. Lee, *J. Electrochem. Soc.*, 2002, **149**, A1058.
- 41 Q. Wang, Z. H. Wen and J. H. Li, *Adv. Funct. Mater.*, 2006, **16**, 2141.
- 42 M. Kaempgen, C. K. Chan, J. Ma, Y. Cui and G. Gruner, *Nano Lett.*, 2009, **9**, 1872.
- 43 L. Kavan and M. Gratzel, *Electrochem. Solid-State Lett.*, 2002, **5**, A39.
- 44 M. M. Thackeray, P. J. Johnson, L. A. Depicciotto, P. G. Bruce and J. B. Goodenough, *Mater. Res. Bull.*, 1984, **19**, 179.
- 45 L. B. Hu, H. Wu, F. La Mantia, Y. A. Yang and Y. Cui, *ACS Nano*, 2010, **4**, 5843.
- 46 J. A. Rogers, T. Someya and Y. G. Huang, *Science*, 2010, **327**, 1603.
- 47 T. Sekitani and T. Someya, *Adv. Mater.*, 2010, **22**, 2228.
- 48 L. B. Hu, W. Yuan, P. Brochu, G. Gruner and Q. B. Pei, *Appl. Phys. Lett.*, 2009, 94.
- 49 L. Hu, H. Wu, F. La Mantia, Y. Yang and Y. Cui, *ACS Nano*, 2010, **4**, 5843–5848.
- 50 L. Hu, W. Chen, X. Xie, N. Liu, Y. Yang, H. Wu, Y. Yao, M. Pasta, H. N. Alshareef and Y. Cui, *ACS Nano*, 2011, **5**, 8904–8913.
- 51 L. Hu, F. La Mantia, H. Wu, X. Xie, J. McDonough, M. Pasta and Y. Cui, *Adv. Energy Mater.*, 2011, **1**, 1012–1017.
- 52 X. Xie, M. Pasta, L. B. Hu, Y. A. Yang, J. McDonough, J. Cha, C. S. Criddle and Y. Cui, *Energy Environ. Sci.*, 2010, **4**, 1293.
- 53 D. T. Schoen, A. P. Schoen, L. B. Hu, H. S. Kim, S. C. Heilshorn and Y. Cui, *Nano Lett.*, 2010, **10**, 3628.
- 54 S. Kalia, B. S. Kaith and I. Kaur, *Cellulose Fibers: Bio- and Nano-Polymer Composites*, Springer, 2011.
- 55 M. B. B. J. Collier and P. G. Tortora, *Understanding Textiles*, Prentice Hall, 2009.